Three isoelectronic families of X4 Y4 cubic systems

Véronique Brumas, Stefano Evangelisti, Nadia Ben Amor

Noname manuscript No.
(will be inserted by the editor)

Three Isoelectronic Families of X_4Y_4 Cubic Systems

Véronique Brumas · Stefano Evangelisti · Nadia Ben Amor

Received: date / Accepted: date

Abstract We performed several types of *ab initio* calculations, from Hartree-Fock to Complete-Active-Space second-order perturbation theory and Coupled Cluster, on compact clusters of stoichiometry X_4Y_4, where X and Y are atoms belonging to the second row of the periodic table. More precisely, we considered the "cubic" structures of three isoelectronic groups, having a total of 48, 52, and 56 electrons, respectively. Notice that the highly symmetric cubic clusters of type X_8 are characterized by an O_h symmetry group, while the X_4Y_4 structures, with X≠Y, have at most a T_d symmetry. Binding energies and wavefunction analysis of these clusters have been performed, in order to investigate the nature, and the electron delocalization of these systems and establish a comparison between them. To this purpose, we also computed the Total-Position Spread tensor for each structure, a quantity which is related to the multi-reference nature of a system wavefunction.

Véronique Brumas · Stefano Evangelisti · Nadia Ben Amor

Laboratoire de Chimie et Physique Quantiques, Université de Toulouse et CNRS, 118, Route de Narbonne, F-31062 Toulouse Cedex - France

E-mail: benamor@irsamc.ups-tlse.fr

1 Introduction

The atoms belonging to the second-row of the periodic table of elements can form compact clusters having remarkable properties. For example, beryllium oxide $(BeO)_n$ clusters have been proposed as a possible material for hydrogen storage, which is being widely studied in the search for renewable energies.[1,2] Manaa[3] mentioned the interesting properties of hexagonal and cubic phases of BN, as extreme hardness, low dielectric constant, large gap and high thermal stability, and the importance of small size clusters in astrophysics, combustion and material science. The cubic BN was also proposed as ultrawide-bandgap semiconductor material.[4] In several studies, cubic species were studied as potential high-energy density materials.[5–7] Spherical aromaticity is a concept that was first used to describe fullerene[8], then later applied to other systems such as the C_8 cubic system, the smallest system that exhibits spherical aromaticity.[9–11,3,12–14] The rule developed by Hirsch and collaborators states that spherical aromaticity occurs when the number of π electrons is equal to $2(n+1)^2$. Several studies can be found in the literature on B_4F_4 clusters.[15–17] However, these structures are not cubic but based on Boron cages, tetrahedral clusters, where each boron atom is bonded to an external fluorine one. Finally, we mention the fact that C_4N_4 mono-layers were proposed as a possible support for LiS batteries [18].

It would be impossible to resume here the existing literature about eight-atom X_4Y_4 cubic clusters. In general, in most of these research works, cubic structures are compared with other geometric arrangements, like the linear, the cyclic, or more exotic ones. We give here a few elements. In 1999, Fowler performed Density Functional Theory Tight Binding (DFTB) and DFT calculations on BN structures. The ring structure was found to be the most stable isomer, with the T_d structure being almost 9.5 eV higher [19]. Martin also found at the Coupled Cluster CCSD(T) level that linear structures tend to be the second most stable structure [20]. More recently, Novikov and coworkers[21] compare the CCSD(T) results to the DFT ones, by comparing the results of 24 exchange-correlation functionals and concluding that B3P86V5 and B97 reproduce the geometry while OP and VWN functionals are more satisfactory for the electronic characteristics. The spherical aromaticity of both cubic C_8 and B_4N_4 was studied at the coupled cluster level[22] and a comparison of these two systems was also published by Jensen[9] at the Moller Plesset perturbation theory (MP2) level and by Manaa[3] at the CCSD and CISD levels. A DFT study on Be_4O_4 structures was done by Ren et al, who performed calculations over rings, double rings, and cages. In particular, the cage was found 1.58 eV higher than the ring [23]. C_4O_4 cyclobutanetetraone was studied at B3LYP, CCSD(T) by Guo in 2012 [24] and by Zhou, Hovrat and Borden [25] (including complete active space perturbation theory (CASPT2) calculations), showing that this form is the most stable one with this stoichiometry. C_4O_4 and N_8 were also studied as novel cubic fuels at the MP2 and Complete-Active-Space Self-Consistent-Field (CASSCF) levels [5,6,26] and later by Schmidt *et al*[7].

It turned out that C_4O_4 has a minimum so shallow that no vibrational states are permitted, while the barrier of cubic N_8 is extremely low, so that the cubic species is predicted to be very unstable [7]. Ochsenfeld and Ahlrichs[27] have studied Li_4F_4 clusters by using HF and Moller Plesset perturbation theory (MP2) methods and, as Lintuluoto,[28] concluded that cubic Li_4F_4 was the most stable structure. In a DFT study[29], one of the aims of the work of Bickelhaupt and co-workers was to better understand the nature of the most polar bond in chemistry, and to distinguish between covalent or ionic features in the bonding mechanism. To our knowledge, there is no scientific literature on the C_4N_4, B_4F_4, Be_4F_4 and B_4O_4 cubic systems.

In this work we concentrate our attention on eight-atom cubic clusters having stoichiometry X_pY_{8-p} with X and Y belonging to the second period of the periodic table, and p is equal to four. They can be divided into three isoelectronic groups, having 48, 52, and 56 electrons, respectively. Their electronic structures range from closed-shell edifices very well described by a single Slater determinant, like for instance N_8, to highly open-shell wavefunctions. These X_4Y_4 species, can have, in principle, a highly symmetric structure with (at most) a T_d symmetry (or O_h, in the case of X_8 clusters). In some cases, however, the system can assume a lower symmetry, C_{2v} or even C_s point group in the case of C_4N_4. In this study, we performed *ab initio* calculations on several types of these "cubic" clusters. We used several types of theoretical methods, starting from Hartree-Fock (HF), and then moving forward in order to add electron correlation. In particular, we used approaches of the family of Coupled-Cluster (CC) for structures that are essentially of a single-reference (SR) type, and whose wavefunction is well described by a single Slater Determinant. If, on the other hand, several determinants are needed in order to describe the system wavefunction, CC approaches are in general unsuitable, and one has to use Multi-Reference (MR) methods: among these, the CASSCF and second-order pertubation theory (CASPT2) approaches are probably the most widespread and good performing. CASSCF adds the non-dynamical correlation due to the most important determinants and then, the remaining dynamical correlation has been be added at a perturbative level, through the CASPT2 procedure.

The present work is organized as follows. In Section 2, thanks to Lewis theory, an extremely simple way of imagining new molecules, structures of the different clusters are illustrated, in order to stress the variety of electronic arrangements. In Section 3, the Total-Position Spread tensor is introduced, and it is shown that this quantity is a powerful indicator of the multireference nature of a wavefunction. For this reason, it can be interesting to compute this tensor for the different structures, compare their behavior, and correlate it to the Lewis structures. The computational details are given in Section 4 while Section 5 presents the detailed results of the electronic-structure calculations performed for this work. Finally, in Section 6 some conclusions are drawn.

2 Cubic Covalent Clusters and Lewis structures

Second-period clusters having a X_4Y_4 structure have a total of 16 core electrons, that do not contribute to the electronic structure of the system. The remaining valence electrons can be used to form the 12 "σ" bonds that characterize the cube structure (for a total of 24 electrons), plus a certain number of electrons having a "π" nature, and distributed on the cubic cage. We stress the fact, however, that the partition between σ and π orbitals, and hence electrons, is to be taken with caution, since this is rigorous for planar systems only. Here, on the contrary, we are dealing with highly curved structures. Three different isoelectronic families of clusters have been considered in the present work (see Figure 1), each one characterized by a different total number of electrons:

1. 48 electrons - These structures have a total of $48-16 = 32$ valence electrons, that can be partitioned into 24 σ electrons and 8 electrons that occupy orbitals having a π nature. In this group we have the C_8, B_4N_4, Be_4O_4, and Li_4F_4 clusters.
2. 52 electrons - A total of $52 - 16 = 36$ valence electrons, 24 of which are σ and 12 π electrons. The clusters C_4N_4, B_4O_4 and Be_4F_4 are found in this group.
3. 56 electrons - A total of $56 - 16 = 40$ valence electrons, 24 of which are σ and 16 π electrons. We find here the last three clusters, N_8, C_4O_4, and B_4F_4.

In principle, several additional families having a smaller number of electrons are also possible, from 24 to 44, each one characterized by a number of electrons multiple of four. These are, however, compounds that tend to form compact structures (with the possible exception of the family having 44 electrons, *i.e.*, B_4C_4, Be_4N_4, and Li_4O_4), characterized by a "metallic" structure. Other families having more electrons would present hypervalent atoms, something that is not compatible with second-period species. For this reason, all these remaining families will not be considered in the present work.

[Fig. 1 about here.]

2.1 Lewis structures

Despite their qualitative description of the bonds in a molecule, Lewis structures can give a very useful information on the bond nature. All the Lewis structures are depicted in Figure 2. In the C_8 cluster, each carbon atom has four valence electrons. In classical aromatic systems, like for example the benzene, a carbon atom forms three sigma bonds with his neighbours and shares the last one in a π orbital. The π orbitals in this case point all in the same direction, and are therefore orthogonal to the same plane. However, systems

having a different topology also exist, like for instance fullerenes, where these π orbitals are not anymore orthogonal to the same plane, and hence the overlap between closest orbitals is not as large as in planar aromatic systems. This is the so-called spherical aromaticity, a concept which appeared with the discovery of the fullerene.[8,10,11,13,14] In a cubic form, the Lewis structure predicts one π electron in each corner of the cube, placed in an orbital pointing outward with respect to the center of the cube. An aromatic behavior can therefore be expected for the C_8 system.[12,14] In B_4N_4, the boron atoms share 3 valence electrons while the nitrogen atoms share 5 valence electrons. In a Lewis representation, nitrogen and boron atoms share 3 electrons to form the σ bonds and it remains 2 electrons on each nitrogen atom which can be placed in the four corners of the cube. In Be_4O_4, each oxygen atom shares 4 electrons with the beryllium, with one dative bond through a donor-acceptor interaction, since the beryllium atom can only form two covalent bonds with its two valence electrons. In the same idea, one can imagine that there are two dative bonds in Li_4F_4, even if the fluorine atom is better described by four lone pairs. In the 48-electrons systems, only the Lewis structure of C_8 possesses one π electron in each corner of the cube while in the three others systems there are four lone pairs in the corners where the more electronegative atoms are located.
The last family, characterized by a total of 56 electrons, has a π lone pair on each atom.Therefore, each atom has an sp^3 hybridization, and these compounds are characterized by a strong closed-shell nature.
On the other hand, the intermediate family, the one having 52 electrons, has formally one π electron per bond, and therefore a strongly open-shell nature. It is therefore expected that four systems (C_8,C_4N_4, B_4O_4 and Be_4F_4) can exhibit an aromatic behavior, as there are the only ones with unpaired electrons.

[Fig. 2 about here.]

3 The Total-Position Spread Tensor

The Total-Position Spread (TPS) tensor, $\mathbf{\Lambda}$, is an extensive property of a molecule as a whole, like the energy, the dipole moment, the polarizability, etc. This rank-two tensor is defined as the second moment cumulant of the total-position operator. Assuming, for simplicity, that a normalized wavefunction $|\Psi\rangle$ describes the system, we have

$$\mathbf{\Lambda} \;=\; \langle\Psi|\hat{\mathbf{R}}^2|\Psi\rangle \;-\; \langle\Psi|\hat{\mathbf{R}}|\Psi\rangle^2 \tag{1}$$

Here $\hat{\mathbf{R}}$ is the Total-Position operator, *i.e.*, the sum of the position of the individual particles,

$$\hat{\mathbf{R}} \;=\; \sum_{\mu} \hat{\mathbf{r}}_{\mu} \tag{2}$$

with the sum going over all the particles of the system (electrons only, in the present case, since we are working in the Born-Oppenheimer approximation). The TPS was introduced several years ago by Resta and co-workers [30–33] under the name of Localization Tensor, which is actually the quantity $\mathbf{\Lambda}$ considered in the present work, divided by the number of electrons present in the system. The Localization Tensor plays a very important role in the theory of electrical conductivity, since its value diverges at the growing of the number of electrons for metallic systems, while it remains finite for insulators. This property of the TPS tensor has been extensively investigated in our group, both in model systems and at an *ab initio* level [34–43].

In a molecular context, like the present one, it is more convenient not to divide the position spread for the total number of the electrons of the system, since it can be shown that the TPS is an additive quantity for a system composed of several non-interacting subsystems. (As a rather technical remark, we notice that this property is true only in absence of entanglement, or non-dynamical correlation, between the different non-interacting subsystems). In a series of papers, we have shown that the TPS can be a very useful tool to describe the character of molecular bonds [44–47].

Moreover, we introduced subsequently the Spin-Partitioned TPS, by splitting the tensor in its four spin components $\mathbf{\Lambda}_{\rho\sigma}$, where ρ and σ are spin variables, whose value can be either α (corresponding to spin projection $\mathrm{S_z} = 1/2$) or β (spin projection $\mathrm{S_z} = -1/2$) [48–50,47]. We have shown that, for a single Slater determinants, we have the relation $\mathbf{\Lambda}_{\alpha\beta} = \mathbf{\Lambda}_{\beta\alpha} = \mathbf{0}$. Moreover, if the determinant is formed by doubly occupied spinorbitals (*i.e.*, it is a closed-shell), we have that $\mathbf{\Lambda}_{\alpha\alpha} = \mathbf{\Lambda}_{\beta\beta}$. For this reason, the quantity $\mathbf{\Lambda}_{\alpha\beta} + \mathbf{\Lambda}_{\beta\alpha}$ is a powerful indicator of the multi-reference character of a wavefunction. An important point is related to the tensor nature of the TPS. This implies that its trace is an invariant, not dependent on the orientation of the molecule in the space. Moreover, the TPS depends only on the system wavefunction as a whole, which means that it is invariant under any orbital transformation. These properties imply that $\mathbf{\Lambda}$ (and also $\mathbf{\Lambda}_{\alpha\alpha}$, $\mathbf{\Lambda}_{\beta\beta}$ and $\mathbf{\Lambda}_{\alpha\beta} + \mathbf{\Lambda}_{\beta\alpha}$) are intrinsic properties of the system. It is a remarkable property of the TPS to represent an intrinsic indicator of the Multi-Reference nature of the wavefunction.

Because of its tensorial nature, the TPS elements depend on the orientation of the system in the space. It is possible to diagonalize the TPS matrix, and extract its eigenvalues and eigenvectors. It should be noticed, however, that for highly symmetric systems (in our case, in particular, T_d and O_h symmetry group), the three eigenvalues are degenerate, and their eigenvectors are not uniquely defined. In order to extract from a TPS its orientation-free information content, it is convenient to compute its trace. The TPS trace is a scalar quantity that is independent of the system's orientation in space. This quantity was computed and reported in the study to provide a measure of the

system's overall behavior. By using the TPS trace, it is possible to obtain information about the system's properties. The TPS trace only will be reported in the present work.

4 Computational Details

Atomic Natural Orbitals (ANO) [51] basis sets, optimized by Roos and coworkers, were used for all atoms in this study. The rather large $(14s9p4d3f)$ uncontracted basis set was contracted to a triple-zeta plus polarization [4s3p2d1f] basis. Although not a very large basis set, this contraction permits to obtain quantitatively reliable results on the light second-row here considered atoms.

All calculations were performed by using the MOLPRO [52,53] and MOLCAS [54–56] quantum-chemistry packages. The optimization of the geometries was performed in the highest possible abelian symmetry point subgroup of the true symmetry group of the system. Therefore, accordingly to the cluster under examination, the calculation has been done in D_{2h}, D_2, C_{2v}, or C_s symmetry. Indeed, we notice that the MOLCAS and MOLPRO packages can deal with only Abelian symmetry groups. Generally speaking, therefore, the O_h cubic symmetry must be lowered to D_{2h}, while the T_d tetrahedric symmetry is reduced to D_2. However, in some cases, there is a symmetry-breaking phenomenon that reduces the system symmetry. All the symmetry point groups are given in the tables and, in parenthesis, the Abelian symmetry groups in which the calculations were performed.

After a preliminary Hartree-Fock calculation, the electron correlation was taken into account by means of Coupled-Cluster (CC) or Complete-Active-Space Self-Consistent-Field (CAS-SCF) [57], followed by CASPT2 calculations [58]. In particular, CC calculations were restricted to Single and Double excitations (CCSD) [59], or also included triple excitations at a perturbative level (CCSD(T)) [60]. The various active spaces included the "π" electrons, *i.e.*, 8 electrons into 8 peripheric orbitals for the 48 isoelectronic group, 4 electrons into 4 orbitals for the 52-electron systems, and finally none for the 56 isoelectronic group since these systems are closed-shells. For C_4N_4, B_4O_4 and Be_4F_4, additional CASPT2 geometry optimizations were performed in order to check the structure and the spin multiplicity of the ground state, since the systems presented a multi-reference character. For these systems, the active space contains 4 electrons in 4 orbitals. At the end of the geometry optimization, and for all considered clusters, the harmonic frequencies were evaluated numerically, in order to check if the optimized geometry corresponded indeed to a local minimum, even if the symmetry constraints are relaxed.

Finally, we notice that all the TPS calculations have been performed on the MOLPRO code, by using the TPS sections inserted in the package for this purpose [61], [62]. At the moment, only the CAS-SCF approach (and hence the HF too) permits the calculation of the spin-summed [61] and spin-partitioned [62] TPS tensors. However, they have been calculated at the CCSD or CCSD(T) geometries.

5 Results

In this section, we summarize the results obtained on the different clusters. We discuss in a first subsection the geometrical structures of the different species, binding energies and natural bond order analysis, and in the following subsection the electronic features (wavefunction, orbital occupation, TPS).

5.1 Structures

Most of the investigated systems present a T_d or O_h symmetry. However, in some cases, the true minimum of the final optimized structure has a lower symmetry than the possible tetrahedral maximum: B_4O_4 and Be_4F_4 belonged to the D_{2d} point group (and they were treated in the C_{2v} Abelian point group) while C_4N_4 was found to be of C_s symmetry only. However, at CASPT2 level, more relevant for open-shell systems, the geometry optimization of C_4N_4 gives a stable D_{2d} structure. The distances and number of imaginary frequencies are given in Tables 1, 2 and 3. The C_8 system presented one imaginary frequency at the CCSD level while it was not the case at the CCSD(T) one. One can note that when the smaller ANO [3s2p1d] basis set is used [22] no imaginary frequency was found, even at the CCSD level while with aug-cc-pVDZ basis set one imaginary frequency was found at the CCSD level and none at the CCSD(T) one [14]. The conclusion [22] was that these instabilities were due to numerical problems in the determination of the frequencies. All the other optimized structures correspond to local minima at both CCSD and CCSD(T) levels at the exception of B_4F_4, the only one for which no local minimum was found, and Be_4F_4 for which the CCSD(T) optimized geometry presents one imaginary frequency. However, it was not the case at the CCSD or CASPT2 level. As already mentioned, C_4N_4, B_4O_4 and Be_4F_4 present a multi-reference character, which means that the CC methods are less suitable than the CASPT2 method.

The distance between first-neighbour atoms (XY distance) varies from 1.44 to 1.84 Å. In each series, this distance increases from the left to the right of the tables, in connection with the increase of the difference of electronegativity between the adjacent atoms. Previous calculations on Li_4F_4 [27–29] give for the XY distance in the Li_4F_4 cubic form values in quite good agreement with our

result (1.835 Å): 1.92 Å(MP2/DZP)[28], 1.824 Å(MP2/6s3p2d Li and 6s5p3d2f for F)[27] and 1.859 Å(DFT-BP86/Slater basis TZP+polarization 3d4f for F and 2p for Li)[29].

Three systems have a particularly long XY distance : Li_4F_4 (1.84 Å), Be_4F_4 (1.71 Å) and B_4F_4 (1.84 Å). The common point is that theses systems involve fluorine atoms and then ionic bonds.

Li_4F_4 can be seen as a cube of lithium atoms inside a larger cube of fluorine atoms as the distance between Li atoms is smaller than the distance between fluorine atoms.[29] Then, the Be-Be (2.5 Å) and B-B (2.8 Å) distances are larger than the Li-Li one, even though the latter has a larger ionic radius and the greatest electronegativity difference with fluorine, leading to the strongest attraction with the fluorine neighbours. This interaction mainly comes from the $2s$ orbital of the lithium with the $2p$ orbital of the fluorine, as for the beryllium atom, with one electron more. The interaction between B and F involves the $2p$ orbitals. However, the optimized cubic structure of B_4F_4 does not correspond to a local minimum.
As expected, the diagonal distances between atoms of the same nature increase when they are bonded to more electronegative atoms. For example, the distance between two boron atoms increases from 1.999 Å in B_4N_4 to 2.503 Å in B_4O_4 and 2.824 Å in B_4F_4. For all systems, the distances calculated at the CCSD(T) level are slightly longer than the CCSD ones. For the multireference 52-electrons series, CASPT2 method was used and the optimized distances are similar to the CCSD ones, with the exception of C_4N_4.

The binding energies given in Table 4 are the difference between the total energy of X_4Y_4 and four times the total energy of the optimized dimer XY. In parenthesis, the XY distances are given. One can first note that the XY distance is much smaller in the dimer than in the X_4Y_4 system (Tables 1-3 and 4). In the 48-electrons series, at the exception of C_8, the XY distance is increased by about +0.23 Å. This increase is about +0.33 Å and +0.42 Å in the 52-electrons and 56-electrons series respectively. The negative calculated binding energies of the two first series with respect to the optimized dimers show that these series are thermodynamically stable or metastable. These binding energies are larger for the 48-electrons series (between -187 and -466 kcal/mol) than for the 52-electrons one (between -52 and -120 kcal/mol). On the contrary, the last 56-electrons series present large positive binding energies and are local minima in the potential energy surface (at the exception of B_4F_4), consequently, this fact has led to the view that they may be good candidates as high-energy density materials [5–7]. The studied cubic clusters present a large spread of different bonding character: they range from bonds having a purely covalent nature (C_8, N_8), to moderately ionic bonds (C_4N_4, C_4O_4), to bonds with a clearly ionic nature (B_4N_4, Li_4F_4, B_4O_4), and ending with strongly ionic bonds in the case of Be_4O_4. This can be seen in Table 5 by the partition of the charges (units of the absolute value of the electronic charge) given by the Loprop population analysis[63]. Indeed, in C_4N_4 and C_4O_4, the Loprop

charges are close to 0.3, while in B_4N_4, Li_4F_4, B_4O_4 and Be_4O_4 the values range between 0.54 and 0.89. In the case of Be_4O_4, the Loprop charge is 1.49, which is comparable to the corresponding value for the BeO dimer, 1.54 Å, in excellent agreement with the value of Zhao and collaborators, in their paper on the nature of the polar covalent bond[64]). The natural bond order (NBO) analysis, given in Table 6, is in fairly good agreement with the Lewis structures shown in figure 2. Lewis structures show dative bonds through donor-acceptor interaction, four for Be_4O_4, B_4O_4 and C_4O_4 and eight for $Li_4F{-}4$, Be_4F_4 and B_4F_4, while NBO analysis shows no difference between dative and σ bonds. In the NBO analysis, Li_4F_4 has no sigma bonds, but only lone pairs. In general, it was necessary for the NBO analysis to modify certain thresholds in order to better separate core electrons and lone pairs. However, the NBO analysis of Be_4F_4 failed to describe core electrons and lone pairs correctly. Concerning the so-called diffuse electrons, corresponding to the π electrons, there is a good agreement with the predicted Lewis structures, even if there are, surprisingly, two π electrons in the B_4N_4 cubic system.

[Table 1 about here.]

[Table 2 about here.]

[Table 3 about here.]

[Table 4 about here.]

[Table 5 about here.]

[Table 6 about here.]

5.2 Total Position Spread and Wave-function analysis

The large HOMO-LUMO gaps ($>$ 8 eV, Tables 1-3) calculated for the 48 and 56-electrons series confirm that these systems are well described by one closed-shell determinant. For the 52-electrons series, open-shell systems, the HOMO-LUMO gap is smaller, between 3.71 and 6.89 eV, at the CASPT2 geometries. One can note that the HOMO-LUMO gap obtained for C_4N_4 at the CCSD(T) geometry is found more than 2 eV above the value calculated at the CASPT2 one.

At the CCSD(T) geometries, the spin-summed TPS calculated at the CASSCF level and presented in Tables 1-3, decreases in each series: from 85 Bohr^2 for C_8 until 43 Bohr^2 for Li_4F_4 (48 electrons), from 84 Bohr^2 for C_4N_4 until 64 Bohr^2 for Be_4F_4 (52 electrons) while this decrease is very small for the 56-electrons series (78.7 to 75.3 Bohr^2). The spin-summed TPS and HOMO-LUMO gap variations are almost linear for the two 48 and 56 electrons series with different slopes (Figure 3). The two curves corresponding to the 56 electrons series are quite flat while the 48 electrons series presents an important slope (-18.7

Bohr^2) for the TPS curve, and a positive slope (2.2 eV) for the HOMO-LUMO gap. The spin-summed total position spread of the 52-electron series is quite similar to the 56-electron series. The value of the spin-partitioned $\alpha\beta + \beta\alpha$ TPS (Tables 1-3 and Figure 4) is close to zero for the three last systems of the 48-electrons series and equal to zero, by definition, for all the closed-shell 56-electrons series. Four systems present a nonzero spin-partitioned $\alpha\beta + \beta\alpha$ TPS, much larger for B_4O_4 (-31.3 Bohr^2) and Be_4F_4 (-52.7 Bohr^2) than for C_8 (-11.9 Bohr^2) and C_4N_4 (-8.0 Bohr^2). As previously mentioned, this is characteristic of a multi-reference wavefunction. The analysis of their CASSCF wavefunction, which is the wavefunction corresponding to the CASPT2 energy, shows that C_8 possesses 8 delocalized electrons on all corner orbitals while B_4O_4 and Be_4F_4 have only 4 single electrons. The active orbitals are depicted in Figures 5-8. They are localized on all the corners for C_8, with a contribution on the CC bonds. In the case of C_4N_4, B_4O_4, and Be_4F_4, for which a CAS(4,4) was used, the molecular orbitals are mainly localized on the 2s orbital of the less electronegative atoms, with a small contribution on the 2p of the nitrogen atoms in the case of C_4N_4. The delocalization is then more important for C_8 and -as for the benzene- the wave function is almost well represented by the Hartree-Fock determinant with a coefficient of 0.8 (weight of 0.64). Indeed, C_8 presents spherical aromaticity, a concept coming from the fullerene discovery[8] and developed in the works of Hirsh[10,12]. In C_4N_4, Be_4F_4 and even more in B_4O_4, the coefficient of Hartree-Fock determinant in the CASSCF wavefunction is smaller: 0.75 (weight 0.56), 0.61 (weight 0.37) and 0.50 (weight 0.25). These wave functions developed on the largest configuration state functions (CSF) coefficients are given below and the corresponding CASSCF molecular orbitals are presented in Fig 5-8:

$$\Psi^{C8} = -0.80|22220000\rangle - 0.18|2ud2ud00\rangle + 0.18|02220002\rangle + 0.17|22022000\rangle - 0.16|22udu0d0\rangle + 0.16|2u2d0ud0\rangle + 0.16|u22d00ud\rangle + 0.15|ud220u0d\rangle + ...$$

At the CASPT2 optimized geometry, the wave function of C_4N_4 is:
$$\Psi^{C4N4} = 0.75|2200\rangle + 0.36|udud\rangle - 0.29|2020\rangle - 0.29|2002\rangle + 0.23|0022\rangle - 0.15|0220\rangle - 0.15|0202\rangle$$

$$\Psi^{B4O4} = 0.61|2200\rangle + 0.38|0022\rangle - 0.29|2020\rangle - 0.29|2002\rangle + 0.48|udud\rangle - 0.20|0220\rangle - 0.20|0202\rangle$$

$$\Psi^{Be4F4} = -0.50|2200\rangle + 0.50|2020\rangle + 0.42|udud\rangle + 0.36|0202\rangle - 0.25|uudd\rangle - 0.36|0022\rangle$$

These 52-electrons systems have a strong multi-radical character. Triplet and quintet states have been calculated at the CASPT2 level and are higher in energy. All the other systems are well represented by one closed-shell determinant

which molecular orbitals corresponding to the "π" orbitals are represented in the SI.

[Fig. 3 about here.]

[Fig. 4 about here.]

[Fig. 5 about here.]

[Fig. 6 about here.]

[Fig. 7 about here.]

[Fig. 8 about here.]

6 Conclusions

We presented a study in which various computational methods were used to investigate compact clusters with a specific stoichiometry: X_4Y_4, where X and Y are atoms from the second row of the periodic table. The clusters were divided into three isoelectronic groups, each containing a different number of electrons (48, 52, and 56). We employed several levels of *ab initio* calculations, including Hartree-Fock, Complete-Active-Space Second-Order Perturbation Theory, and Coupled Cluster, in order to analyze the properties of these clusters. The aim of the study was to gain a better understanding of the nature of the wavefunction associated with these structures.

The clusters were found to have a generally cubic shape, with highly symmetric structures of type X_8 exhibiting the maximum possible symmetry, *i.e.*, an O_h symmetry group. The X_4Y_4 structures with X$\neq$Y, on the other hand, have at most a T_d symmetry. With the exception of the B_4F_4 cluster, all the optimized structures correspond to local minima. In all cases, the calculated distances are substantially larger than in the XY, dimer and increase with the difference of electronegativity between X and Y. The binding energies were calculated with respect to the XY dimer and show that the 48 and 52-electrons series are thermodynamically stable. On the contrary, the structures belonging to the 56-electrons series are strongly exothermic. Two systems of this latter series correspond to local minima and have been identified as possible candidates as high-energy density materials [5–7]. The natural bond order analysis is in rather good agreement with the predicted structures by Lewis theory. The wavefunction analysis has shown the multi-radical character of the 52-electrons series and the aromaticity of the C_8 allotrope of carbon. As a complement to the investigation of the wavefunction nature of the clusters, we computed the Total-Position Spread tensor for each structure. This quantity is related to the multi-reference nature of these systems, and its calculation

provides insight into the behavior of the electrons within the cluster. In particular, the behavior of the spin-partitioned TPS tensor is strongly related to the presence of correlation in the systems, since the mixed-spin components vanish for a single Slater determinants. The 52-electron series shows a strong multi-reference character, and this feature significantly increases by going from C_4N_4 to Be_4F_4. On the other hand, the two other series, the 48- and 56-electron ones, are essentially closed-shell nature, and qualitatively well described by a single Slater determinant.

We believe that the study of these systems gives an interesting insight into the properties of these compact clusters and advances our understanding of their wavefunction and electronic structure.

Acknowledgments

It is a real pleasure for us to dedicate this work to our friend and colleague, Prof. Maurizio Persico, in honor of his 70th birthday.

This work was partly supported by the French "Centre National de la Recherche Scientifique" (CNRS, also under the PICS action 4263). It has received fundings from the European Union's Horizon 2020 research and innovation program under the Marie Skłodowska-Curie grant agreement n°642294. This work was also supported by the "Programme Investissements d'Avenir" under the program ANR-11-IDEX-0002-02, reference ANR-10-LABX-0037-NEXT.

References

1. R. Shinde and M. Tayade, "Remarkable Hydrogen Storage on Beryllium Oxide Clusters: First-Principles Calculations," The Journal of Physical Chemistry C, vol. 118, pp. 17200–17204, Aug. 2014.
2. O. Roberto-Neto and E. F. V. de Carvalho, "A DFT and wave function theory study of hydrogen adsorption on small beryllium oxide clusters," Theoretical Chemistry Accounts, vol. 139, p. 93, May 2020.
3. M. Manaa, "A comparative study of cubic B4N4 and C8," Journal of Molecular Structure: THEOCHEM, vol. 549, pp. 23–26, Aug. 2001.
4. J. Y. Tsao, S. Chowdhury, M. A. Hollis, D. Jena, N. M. Johnson, K. A. Jones, R. J. Kaplar, S. Rajan, C. G. Van De Walle, E. Bellotti, C. L. Chua, R. Collazo, M. E. Coltrin, J. A. Cooper, K. R. Evans, S. Graham, T. A. Grotjohn, E. R. Heller, M. Higashiwaki, M. S. Islam, P. W. Juodawlkis, M. A. Khan, A. D. Koehler, J. H. Leach, U. K. Mishra, R. J. Nemanich, R. C. N. Pilawa-Podgurski, J. B. Shealy, Z. Sitar, M. J. Tadjer, A. F. Witulski, M. Wraback, and J. A. Simmons, "Ultrawide-Bandgap Semiconductors: Research Opportunities and Challenges," Advanced Electronic Materials, vol. 4, p. 1600501, Jan. 2018.
5. S. Evangelisti, "Ab initio study of C4O4 in Td symmetry," Chemical Physics Letters, vol. 259, pp. 261–264, Sept. 1996.
6. S. Evangelisti, "Carbon-oxygen clusters as hypothetical high energy-density materials," Chemical Physics, vol. 218, pp. 21–30, May 1997.
7. M. W. Schmidt, M. S. Gordon, and J. A. Boatz, "Cubic fuels?," Int. J.Quant. Chem., vol. 76, no. 3, pp. 434–446, 2000.
8. H. W. Kroto, J. R. Heath, S. C. O'Brien, R. F. Curl, and R. E. Smalley, "C60: Buckminsterfullerene," Nature, vol. 318, p. 162, Nov. 1985.
9. F. Jensen, "The stability of cage and ring isomers for carbon and boron nitride clusters," Chemical Physics Letters, vol. 209, pp. 417–422, July 1993.
10. A. Hirsch, Z. Chen, and H. Jiao, "Spherical Aromaticity inIh Symmetrical Fullerenes: The 2(N+1)2 Rule," Angewandte Chemie, vol. 39, pp. 3915–3917, Nov. 2000.
11. M. Bühl and A. Hirsch, "Spherical Aromaticity of Fullerenes," Chem. Rev., vol. 101, pp. 1153–1184, May 2001.
12. A. Hirsch, "The era of carbon allotropes," Nature Materials, vol. 9, pp. 868–871, Nov. 2010.
13. J. Poater and M. Sola, "Open-shell spherical aromaticity: the 2n2 + 2n + 1 (with s = n + 1/2) rule," Chem. Commun., vol. 47, pp. 11647–11649, 2011.
14. D. Sharapa, A. Hirsch, B. Meyer, and T. Clark, "Cubic C $_8$: An Observable Allotrope of Carbon?," ChemPhysChem, vol. 16, pp. 2165–2171, July 2015.

15. M. F. Guest and I. H. Hillier, "Electronic structure of boron hydrides. Ab initio study of $B_{10}H_{14}$, $B_{10}H_{14}^{-2}$, and $B_{10}H_{12}^{-2}$," Journal of the Chemical Society, Faraday Transactions 2, vol. 70, p. 2004, 1974.

16. C.-S. L. Lin and C.-W. J. Liu, "Theoretical study on tetranuclear boron clusters: B_4X_4 (X = H, F, Cl, Br, I)," Chinese Journal of Chemistry, vol. 12, pp. 305–313, Aug. 2010.

17. D. J. Swanton and R. Ahlrichs, "Electronic structures of the boron cage molecules B4H4, B4Cl4 and B4F4," Theoretica Chimica Acta, vol. 75, no. 3, pp. 163–172, 1989.

18. T. Li, C. He, and W. Zhang, "A novel porous C_4N_4 monolayer as a potential anchoring material for lithium–sulfur battery design," Journal of Materials Chemistry A, vol. 7, no. 8, pp. 4134–4144, 2019.

19. P. W. Fowler, K. M. Rogers, T. Heine, and G. Seifert, "Homonuclear bonds in BN clusters?," in The 13th international winterschool on electronic properties of novel materials- science and technology of molecular nanostructures, (Kirchberg, Tirol (Austria)), pp. 170–174, ASCE, 1999.

20. J. M. Martin, J. El-Yazal, J.-P. François, and R. Gijbels, "Structures and thermochemistry of B_3N_3 and B_4N_4," Chemical Physics Letters, vol. 232, pp. 289–294, Jan. 1995.

21. N. V. Novikov, I. Y. Dolinskiy, M. A. Gimaldinova, K. P. Katin, and M. M. Maslov, "Benchmark study of the exchange-corrected density functionals: Application to strained boron nitride clusters," Turkish Computational and Theoretical Chemistry, vol. 1, no. 2, pp. 27 – 34, 2017.

22. B. Chaglayan, A. W. Huran, N. Ben Amor, V. Brumas, S. Evangelisti, and T. Leininger, "Spherical aromaticity and electron delocalization in C_8 and C_4N_4 cubic systems," Theoretical Chemistry Accounts, vol. 138, no. 1, 2019.

23. L. Ren, L. Cheng, Y. Feng, and X. Wang, "Geometric and electronic structures of $(beo)_n$ (N = 2–12, 16, 20, and 24): Rings, double rings, and cages," The Journal of Chemical Physics, vol. 137, p. 014309, July 2012.

24. J.-C. Guo, G.-L. Hou, S.-D. Li, and X.-B. Wang, "Probing the Low-Lying Electronic States of Cyclobutanetetraone (C_4O_4) and Its Radical Anion: A Low-Temperature Anion Photoelectron Spectroscopic Approach," The Journal of Physical Chemistry Letters, vol. 3, pp. 304–308, Feb. 2012.

25. X. Zhou, D. A. Hrovat, and W. T. Borden, "Calculations of the Relative Energies of the $^2B_{1g}$ and $^2A_{2u}$ States of Cyclobutanetetraone Radical Cation and Radical Anion Provide Further Evidence of a ^{3} B $_{2u}$ Ground State for the Neutral Molecule: A Proposed Experimental Test of the Prediction of a Triplet Ground State for (CO) $_4$," The Journal of Physical Chemistry A, vol. 114, pp. 1304–1308, Jan. 2010.

26. S. Evangelisti and L. Gagliardi, "A complete active-space self-consistent-field study on cubic N8," Il Nuovo Cimento D, vol. 18, pp. 1395–1405, Dec. 1996.

27. C. Ochsenfeld and R. Ahlrichs, "An ab initio investigation of structure and energetics of clusters KnCln and LinFn," Berichte der Bunsengesellschaft für physikalische Chemie, vol. 98, pp. 34–47, Jan. 1994.
28. M. Lintuluoto, "Theoretical study on the structure and energetics of alkali halide clusters," Journal of Molecular Structure: THEOCHEM, vol. 540, no. 1, pp. 177–192, 2001.
29. F. M. Bickelhaupt, M. Solà, and C. F. Guerra, "Covalent *versus* ionic bonding in alkalimetal fluoride oligomers," Journal of Computational Chemistry, vol. 28, no. 1, pp. 238–250, 2007.
30. R. Resta and S. Sorella, "Electron localization in the insulating state," Phys. Rev. Lett., vol. 82, pp. 370–373, Jan 1999.
31. R. Resta and S. Sorella, "Electron localization in the insulating state," Phys. Rev. Lett., vol. 82, pp. 370–373, Jan 1999.
32. R. Resta, "Quantum-mechanical position operator in extended systems," Phys. Rev. Lett., vol. 80, pp. 1800–1803, Mar 1998.
33. R. Resta, "Why are insulators insulating and metals conducting?," Journal of Physics: Condensed Matter, vol. 14, pp. R625–R656, may 2002.
34. V. Vetere, A. Monari, G. L. Bendazzoli, S. Evangelisti, and B. Paulus, "Full configuration interaction study of the metal-insulator transition in model systems: LiN linear chains (N=2,4,6,8)," The Journal of Chemical Physics, vol. 128, p. 024701, Jan. 2008.
35. A. Monari, G. L. Bendazzoli, and S. Evangelisti, "The metal-insulator transition in dimerized Hückel chains," The Journal of Chemical Physics, vol. 129, p. 134104, Oct. 2008.
36. G. L. Bendazzoli, S. Evangelisti, A. Monari, and R. Resta, "Kohn's localization in the insulating state: One-dimensional lattices, crystalline versus disordered," The Journal of Chemical Physics, vol. 133, p. 064703, Aug. 2010.
37. G. L. Bendazzoli, S. Evangelisti, and A. Monari, "Full-configuration-interaction study of the metal-insulator transition in a model system: H $_n$ linear chains n =4, 6,. . . , 16," International Journal of Quantum Chemistry, vol. 111, pp. 3416–3423, Nov. 2011.
38. G. L. Bendazzoli, S. Evangelisti, and A. Monari, "Asymptotic analysis of the localization spread and polarizability of 1-D noninteracting electrons," International Journal of Quantum Chemistry, vol. 112, pp. 653–664, Feb. 2012.
39. E. Giner, G. L. Bendazzoli, S. Evangelisti, and A. Monari, "Full-configuration-interaction study of the metal-insulator transition in model systems: Peierls dimerization in H n rings and chains," The Journal of Chemical Physics, vol. 138, p. 074315, Feb. 2013.
40. A. Diaz-Marquez, S. Battaglia, G. L. Bendazzoli, S. Evangelisti, T. Leininger, and J. A. Berger, "Signatures of Wigner localization in one-dimensional systems," The Journal of Chemical Physics, vol. 148, p. 124103, Mar. 2018.
41. E. Valença Ferreira De Aragão, D. Moreno, S. Battaglia, G. L. Bendazzoli, S. Evangelisti, T. Leininger, N. Suaud, and J. A. Berger, "A simple position operator for periodic systems," Physical Review B, vol. 99, p. 205144, May 2019.

42. C. Angeli, G. L. Bendazzoli, S. Evangelisti, and J. A. Berger, "The localization spread and polarizability of rings and periodic chains," The Journal of Chemical Physics, vol. 155, p. 124107, Sept. 2021.
43. G. François, C. Angeli, G. L. Bendazzoli, V. Brumas, S. Evangelisti, and J. A. Berger, "Mapping of Hückel zigzag carbon nanotubes onto independent polyene chains: Application to periodic nanotubes," The Journal of Chemical Physics, vol. 159, p. 094106, Sept. 2023.
44. C. Angeli, G. L. Bendazzoli, and S. Evangelisti, "The localization tensor for the H2 molecule: Closed formulae for the Heitler-London and related wavefunctions and comparison with full configuration interaction," The Journal of Chemical Physics, vol. 138, p. 054314, Feb. 2013.
45. O. Brea, M. El Khatib, C. Angeli, G. L. Bendazzoli, S. Evangelisti, and T. Leininger, "Behavior of the Position–Spread Tensor in Diatomic Systems," Journal of Chemical Theory and Computation, vol. 9, pp. 5286–5295, Dec. 2013.
46. G. L. Bendazzoli, M. El Khatib, S. Evangelisti, and T. Leininger, "The total Position Spread in mixed-valence compounds: A study on the model system," Journal of Computational Chemistry, vol. 35, pp. 802–808, Apr. 2014.
47. O. Brea, M. El Khatib, G. L. Bendazzoli, S. Evangelisti, T. Leininger, and C. Angeli, "The Spin-Partitioned Total-Position Spread Tensor: An Application To Diatomic Molecules," The Journal of Physical Chemistry A, vol. 120, pp. 5230–5238, July 2016.
48. M. El Khatib, O. Brea, E. Fertitta, G. L. Bendazzoli, S. Evangelisti, T. Leininger, and B. Paulus, "Spin delocalization in hydrogen chains described with the spin-partitioned total position-spread tensor," Theoretical Chemistry Accounts, vol. 134, p. 29, Mar. 2015.
49. M. El Khatib, O. Brea, E. Fertitta, G. L. Bendazzoli, S. Evangelisti, and T. Leininger, "The total position-spread tensor: Spin partition," The Journal of Chemical Physics, vol. 142, p. 094113, Mar. 2015.
50. E. Fertitta, M. El Khatib, G. L. Bendazzoli, B. Paulus, S. Evangelisti, and T. Leininger, "The spin-partitioned total position-spread tensor: An application to Heisenberg spin chains," The Journal of Chemical Physics, vol. 143, p. 244308, Dec. 2015.
51. P.-O. Widmark, P.-Å. Malmqvist, and B. O. Roos, "Density matrix averaged atomic natural orbital (ANO) basis sets for correlated molecular wave functions: I. first row atoms," Theor. Chim. Acta, vol. 77, no. 5, pp. 291–306, 1990.
52. F. Eckert, P. Pulay, and H.-J. Werner, "Ab initio geometry optimization for large molecules," J. Comput. Chem., vol. 18, no. 12, pp. 1473–1483, 1997.
53. H.-J. Werner, P. J. Knowles, P. Celani, W. Györffy, A. Hesselmann, D. Kats, G. Knizia, A. Köhn, T. Korona, D. Kreplin, R. Lindh, Q. Ma, F. R. Manby, A. Mitrushenkov, G. Rauhut, M. Schütz, K. R. Shamasundar, T. B. Adler, R. D. Amos, S. J. Bennie, A. Bernhardsson, A. Berning, J. A. Black, P. J. Bygrave, R. Cimiraglia, D. L. Cooper,

D. Coughtrie, M. J. O. Deegan, A. J. Dobbyn, K. Doll, M. Dornbach, F. Eckert, S. Erfort, E. Goll, C. Hampel, G. Hetzer, J. G. Hill, M. Hodges, T. Hrenar, G. Jansen, C. Köppl, C. Kollmar, S. J. R. Lee, Y. Liu, A. W. Lloyd, R. A. Mata, A. J. May, B. Mussard, S. J. McNicholas, W. Meyer, T. F. Miller III, M. E. Mura, A. Nicklass, D. P. O'Neill, P. Palmieri, D. Peng, K. A. Peterson, K. Pflüger, R. Pitzer, I. Polyak, M. Reiher, J. O. Richardson, J. B. Robinson, B. Schröder, M. Schwilk, T. Shiozaki, M. Sibaev, H. Stoll, A. J. Stone, R. Tarroni, T. Thorsteinsson, J. Toulouse, M. Wang, M. Welborn, and B. Ziegler, "Molpro, version , a package of ab initio programs." see https://www.molpro.net.

54. F. Aquilante, L. De Vico, N. Ferré, G. Ghigo, P.-å. Malmqvist, P. Neogrády, T. B. Pedersen, M. Pitoňák, M. Reiher, B. O. Roos, L. Serrano-Andrés, M. Urban, V. Veryazov, and R. Lindh, "Molcas 7: The next generation," J. Comput. Chem., vol. 31, no. 1, pp. 224–247, 2010.
55. V. Veryazov, P.-O. Widmark, L. Serrano-Andrés, R. Lindh, and B. O. Roos, "2molcas as a development platform for quantum chemistry software," Int. J. Quantum Chem., vol. 100, no. 4, pp. 626–635, 2004.
56. G. Karlström, R. Lindh, P.-Å. Malmqvist, B. O. Roos, U. Ryde, V. Veryazov, P.-O. Widmark, M. Cossi, B. Schimmelpfennig, P. Neogrady, and L. Seijo, "Molcas: a program package for computational chemistry," Comput. Mat. Science, vol. 28, pp. 222–239, 10 2003.
57. B. O. Roos, P. R. Taylor, and P. E. Siegbahn, "A complete active space SCF method (CASSCF) using a density matrix formulated super-CI approach," Chem. Phys., vol. 48, no. 2, pp. 157–173, 1980.
58. K. Andersson, P. A. Malmqvist, B. O. Roos, A. J. Sadlej, and K. Wolinski, "Second-order perturbation theory with a CASSCF reference function," J. Phys. Chem., vol. 94, pp. 5483–5488, July 1990.
59. C. Hampel, K. A. Peterson, and H.-J. Werner, "A comparison of the efficiency and accuracy of the quadratic configuration interaction (QCISD), coupled cluster (CCSD), and Brueckner coupled cluster (BCCD) methods," Chem. Phys. Lett., vol. 190, pp. 1–12, Feb. 1992.
60. J. D. Watts, J. Gauss, and R. J. Bartlett, "Coupled–cluster methods with noniterative triple excitations for restricted open–shell Hartree–Fock and other general single determinant reference functions. Energies and analytical gradients," J. Chem. Phys., vol. 98, pp. 8718–8733, June 1993.
61. M. El Khatib, T. Leininger, G. L. Bendazzoli, and S. Evangelisti, "Computing the position-spread tensor in the cas-scf formalism," Chem. Phys. Lett., vol. 591, pp. 58–63, 2014.
62. A. W. Huran, T. Leininger, G. L. Bendazzoli, and S. Evangelisti, "Computing the position-spread tensor in the cas-scf formalism ii: Spin partition," Chem. Phys. Lett.,

vol. 664, pp. 120–126, 2016.

63. L. Gagliardi, R. Lindh, and G. Karlström, "Local properties of quantum chemical systems: The LoProp approach," The Journal of Chemical Physics, vol. 121, pp. 4494–4500, Sept. 2004.
64. L. Zhao, S. Pan, and G. Frenking, "The nature of the polar covalent bond," The Journal of Chemical Physics, vol. 157, p. 034105, July 2022.

List of Figures

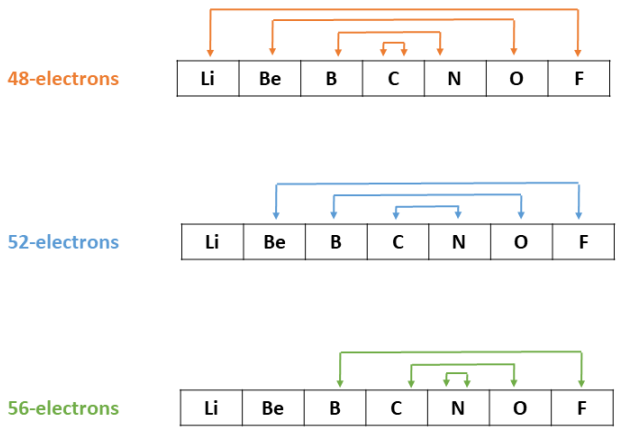

Fig. 1 The construction of the three families of isoelectronic structures from the second period elements of the periodic table.

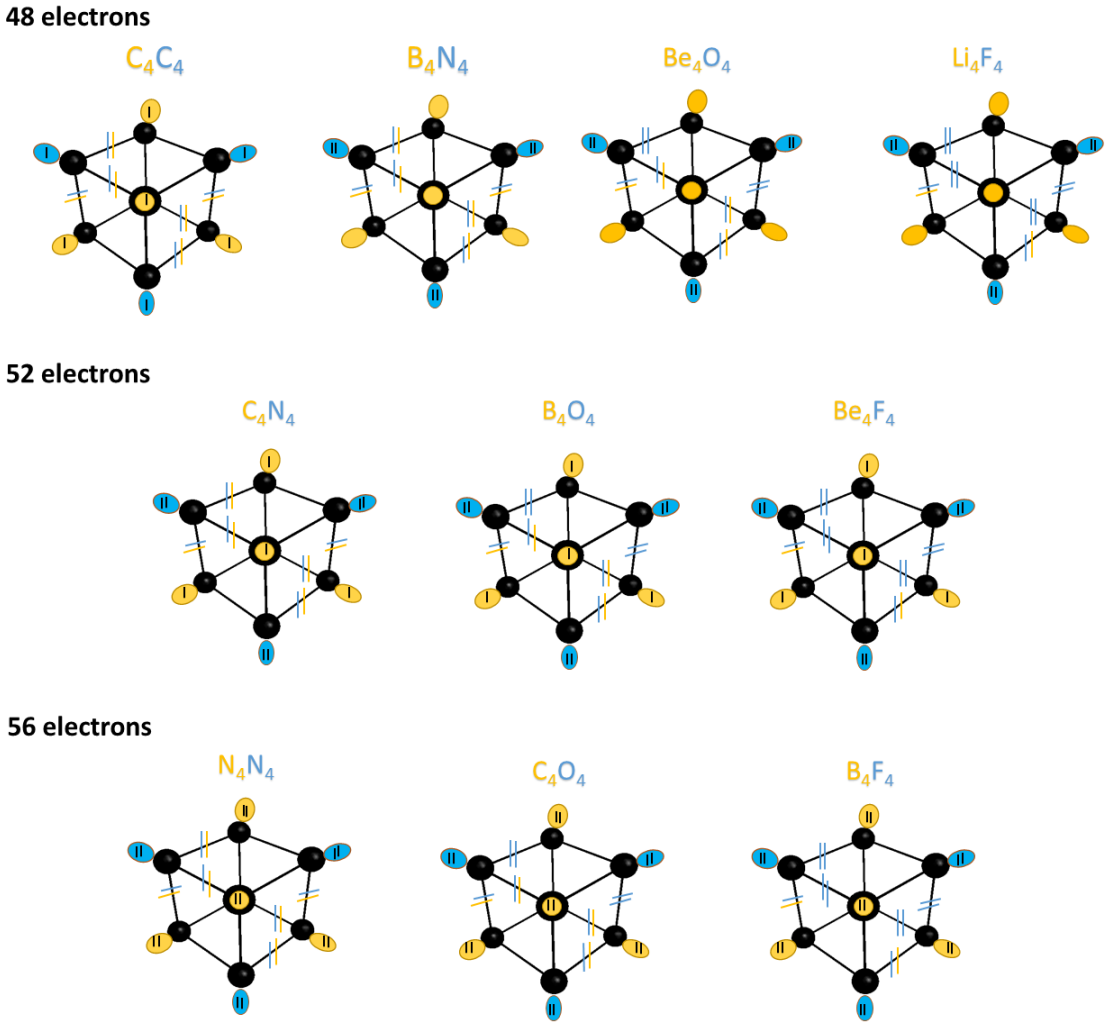

Fig. 2 Lewis structures: the three families of isoelectronic structures are shown. Yellow (X) and blue (Y) colors are used to represent electrons or orbitals of X and Y atoms. For the sake of clarity, the electronic structures around only one X and its opposite Y atom are depicted: the shared electrons in yellow/blue while all the π electrons are represented in black, in yellow/blue orbitals. A double blue bar stands for lone pair from atom X. Notice that a blue orbital is hidden behind the central yellow one in each figure.

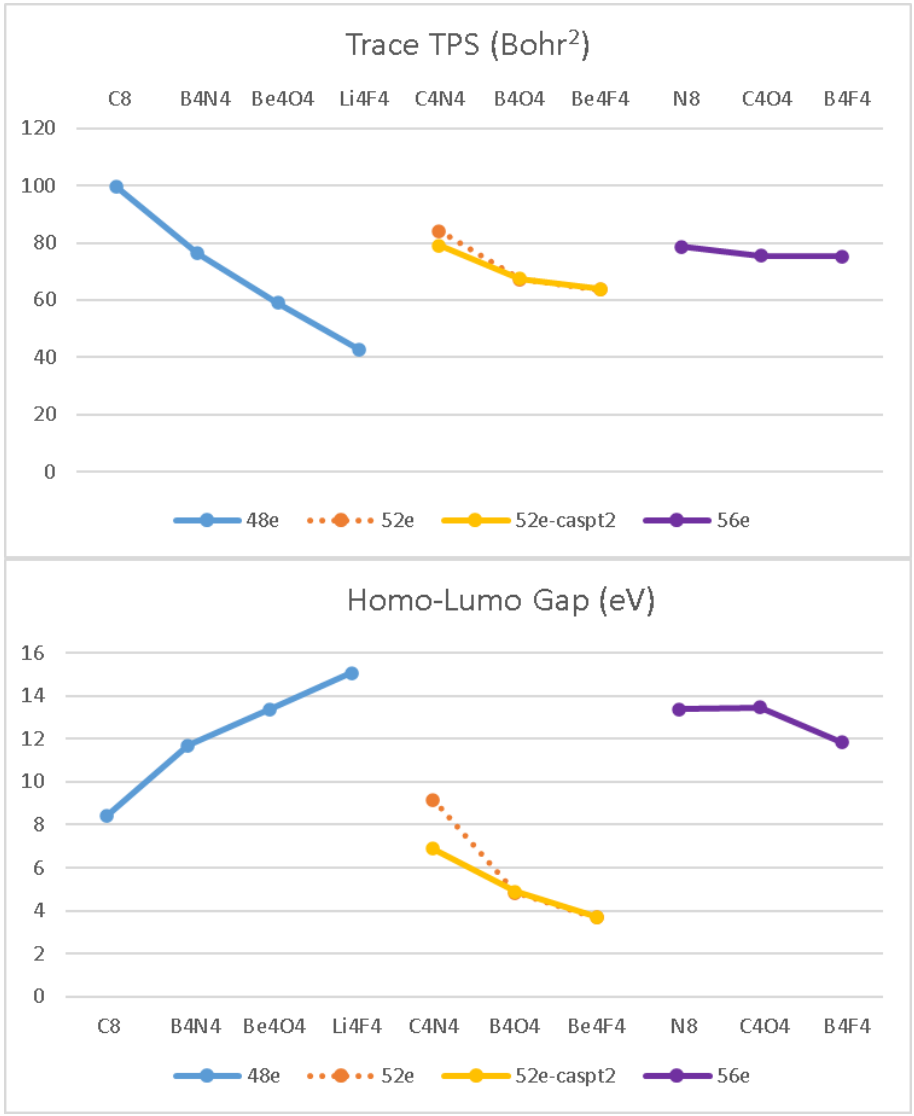

Fig. 3 At the CCSD(T) or CASPT2 geometries:
Top: Spin-summed Total Position Spread (Bohr^2).
Bottom: HOMO-LUMO gap (eV)

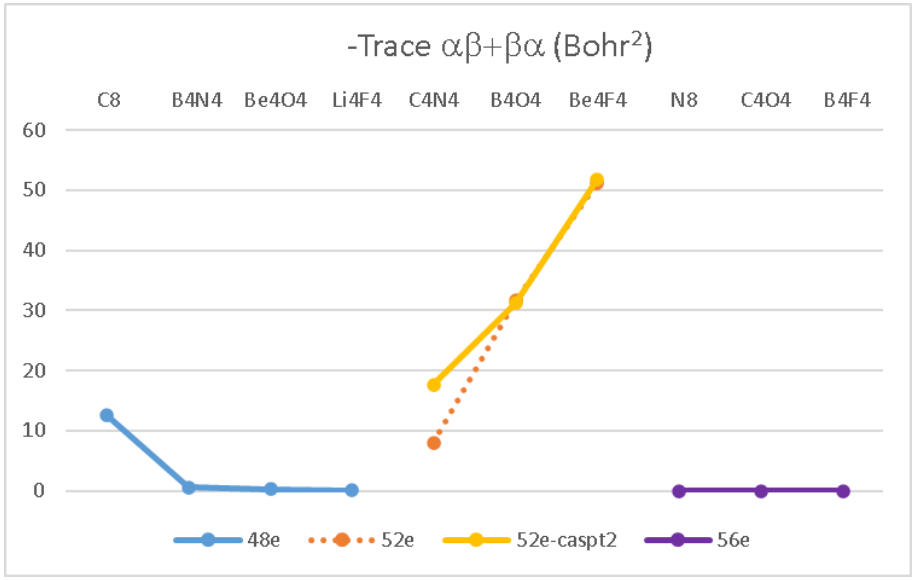

Fig. 4 Spin-partitioned term of the Total Position Spread (Bohr^2) at the CCSD(T) or CASPT2 geometries

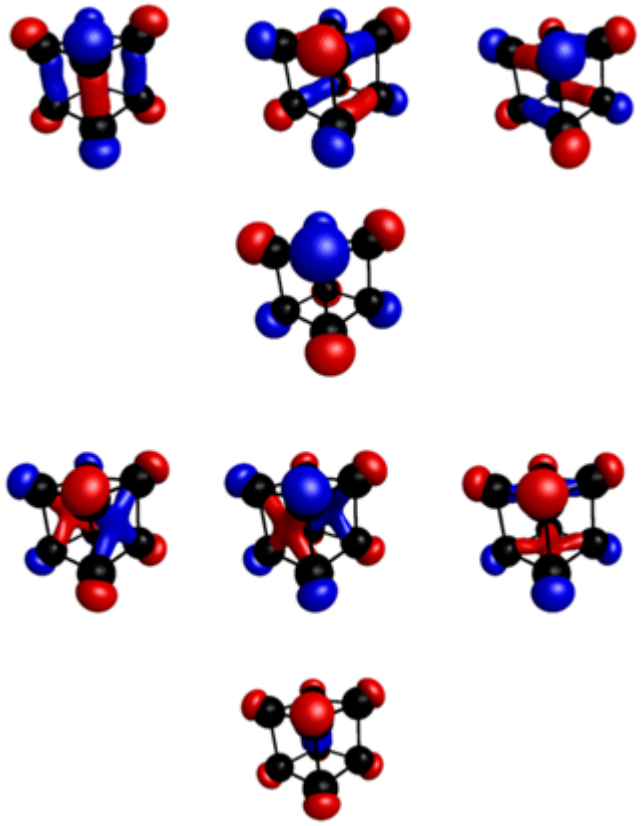

Fig. 5 CASSCF(8,8) molecular orbitals of C_8 (48 electrons).

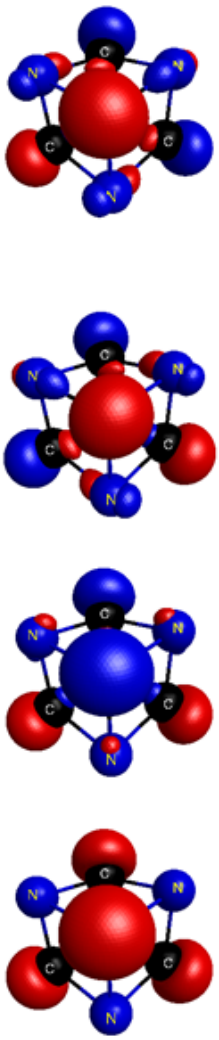

Fig. 6 CASSCF(4,4) molecular orbitals of C_4N_4 (52 electrons).

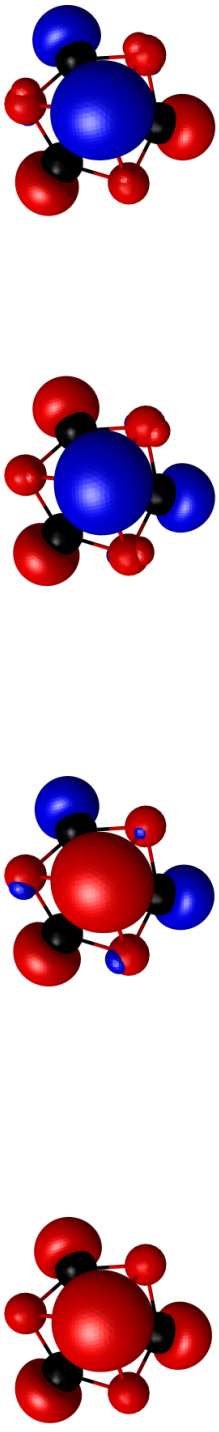

Fig. 7 CASSCF(4,4) molecular orbitals of B_4O_4 (52 electrons).

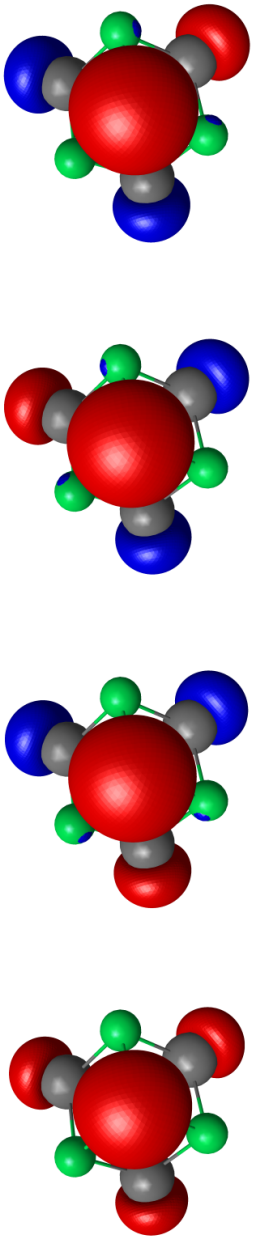

Fig. 8 CASSCF(4,4) molecular orbitals of Be_4F_4 (52 electrons).

List of Tables

Table 1 X_4Y_4 systems with 48 electrons (C_8, B_4N_4, Be_4O_4 and Li_4F_4). ANO-L 4s3p2d1f basis set. The calculations were performed in the Abelian point group given in parenthesis.

CCSD	**C_8** Oh (D2h)	**B_4N_4** Td (D2)	**Be_4O_4** Td (D2)	**Li_4F_4** Td (D2)
Distances (Å)				
d_{XX}	2.083	1.843	1.994	2.439
d_{YY}	2.083	2.360	2.455	2.725
d_{XY}	1.473	1.508	1.590	1.831
Imag. Freq.	1	0	0	0
E_{CCSD} (a.u.)	-303.551296	-317.701338	-359.701547	-429.369980
Trace TPS (Bohr^2)	83.9	76.5	58.8	43.16
Trace $\alpha\alpha + \beta\beta$	95.9	76.7	59.1	43.21
Trace $\alpha\beta + \beta\alpha$	-11.9	-0.27	-0.30	-0.05
HOMO-LUMO gap (eV)	8.65	11.78	13.41	15.09

CCSD(T)	**C_8** Oh (D2h)	**B_4N_4** Td (D2)	**Be_4O_4** Td (D2)	**Li_4F_4** Td (D2)
Distances (Å)				
d_{XX}	2.103	1.851	1.999	2.445
d_{YY}	2.103	2.371	2.464	2.730
d_{XY}	1.487	1.515	1.595	1.835
Imag. Freq.	0	0	0	0
$E_{CCSD(T)}$ (a.u.)	-303.661138	-317.769833	-359.748889	-429.401969
Trace TPS (Bohr^2)	84.7	76.4	59.0	43.20
Trace $\alpha\alpha + \beta\beta$	97.1	77.0	59.3	43.25
Trace $\alpha\beta + \beta\alpha$	-12.5	-0.6	-0.30	-0.05
HOMO-LUMO gap (eV)	8.40	11.70	13.39	15.08

Table 2 X_4Y_4 systems with 52 electrons (C_4N_4, B_4O_4, and Be_4F_4). ANO-L 4s3p2d1f basis set. The calculations were performed in the Abelian point group given in parenthesis.

CCSD	C_4N_4 C3v (Cs)	B_4O_4 D2d (C2v)	Be_4F_4 D2d (C2v)
Distances (Å)			
d_{XX}	2.183 and 2.283	2.089 and 2.081 (2)	2.453 and 2.521 (2)
d_{YY}	1.834 and 2.180	2.235 and 2.275 (2)	2.337 and 2.319 (2)
d_{XY}	1.431, 1.515 and 1.663	1.553 and 1.532 (2)	1.729 and 1.697 (2)
Imag. Freq.	0	0	0
E_{CCSD} (a.u.)	-370.228096	-399.530026	-457.856038
Trace TPS (Bohr^2)	83.5	67.1	63.7
Trace $\alpha\alpha + \beta\beta$	90.4	98.4	116.4
Trace $\alpha\beta + \beta\alpha$	-6.9	-31.3	-52.7
HOMO-LUMO gap (eV)	9.17	4.89	3.78

CCSD(T)	C_4N_4 C3v (Cs)	B_4O_4 D2d (C2v)	Be_4F_4 D2d (C2v)
Distances (Å)			
d_{XX}	2.188 and 2.288	2.110 and 2.094 (2)	2.520 and 2.495 (2)
d_{YY}	1.871 and 2.209	2.261 and 2.273 (2)	2.326 and 2.340 (2)
d_{XY}	1.442, 1.529 and 1.677	1.544 and 1.548 (2)	1.708 and 1.715 (2)
Imag. Freq.	0	0	1
$E_{CCSD(T)}$ (a.u.)	-370.334796	-399.645335	-457.930381
Trace TPS (Bohr^2)	84.1	67.4	63.8
Trace $\alpha\alpha + \beta\beta$	92.1	98.8	114.3
Trace $\alpha\beta + \beta\alpha$	-8.0	-31.4	-50.5
HOMO-LUMO gap (eV)	9.17	4.85	3.63

CASPT2	C_4N_4 D2d (C2v)	B_4O_4 D2d (C2v)	Be_4F_4 D2d (C2v)
Distances (Å)			
d_{XX}	2.074 and 1.962 (2)	2.096 and 2.087 (2)	2.489 and 2.515 (2)
d_{YY}	2.235 and 2.243 (2)	2.261 and 2.283 (2)	2.345 and 2.339 (2)
d_{XY}	1.450 and 1.531 (2)	1.551 and 1.544 (2)	1.725 and 1.711 (2)
Imag. Freq.	0	0	0
HOMO-LUMO gap (eV)	6.89	4.89	3.71

Table 3 X_4Y_4 systems with 56 electrons (N_8, C_4O_4 and B_4F_4). ANO-L 4s3p2d1f basis set. The calculations were performed in the Abelian point group given in parenthesis.

CCSD	N_8 Oh (D2h)	C_4O_4 Td (D2)	B_4F_4 Td (D2)
Distances (Å)			
d_{XX}	2.132	2.224	2.817
d_{YY}	2.132	2.152	2.329
d_{XY}	1.507	1.548	1.836
Imag. Freq.	0	0	5
E_{CCSD} (a.u.)	-436.703278	-452.009010	-497.691637
Trace TPS (Bohr^2)	77.15	74.54	75.11
HOMO-LUMO gap (eV)	13.49	13.48	11.83

CCSD(T)	N_8 Oh (D2h)	C_4O_4 Td (D2)	B_4F_4 Td (D2)
Distances (Å)			
d_{XX}	2.159	2.246	2.824
d_{YY}	2.159	2.177	2.348
d_{XY}	1.527	1.564	1.844
Imag. Freq.	0	0	5
$E_{CCSD(T)}$ (a.u.)	-436.798862	-452.093896	-497.753100
Trace TPS (Bohr^2)	78.65	75.53	75.27
HOMO-LUMO gap (eV)	13.38	13.46	11.85

	E(X4Y4)-4*E(XY)
C_8	-341.2 (1.258)
B_4N_4	-453.5 (1.282)
Be_4O_4	-466.4 (1.352)
Li_4F_4	-187.4 (1.590)
C_4N_4	-52.6 (1.184)
B_4O_4	-120.6 (1.224)
Be_4F_4	-62.4 (1.378)
N_8	425.6 (1.107)
C_4O_4	326.9 (1.139)
B_4F_4	168.0 (1.285)

Table 4 Cohesion energies in kcal.mol^{-1} and, in parenthesis, the XY distance in the dimer in Å. All the values were calculated at the CCSD(T)/ANO-L 4s3p2d1f level (geometries and energies). Zero point energy not taking into account.

	Loprop	Mulliken
C_8	0 / 0	0 / 0
B_4N_4	+0.61 / -0.61	-0.12 / +0.12
Be_4O_4	+1.49 / -1.49	+0.69 / -0.69
Li_4F_4	+0.87 / -0.87	+0.79 / -0.79
C_4N_4	+0.33 / -0.33	+0.38 / -0.38
B_4O_4	+0.54/-0.54	+0.21 / -0.21
Be_4F_4	+0.89 / -0.89	+0.43 / -0.43
N_8	0 / 0	0 / 0
C_4O_4	+0.31 / -0.31	+0.51 / -0.51
B_4F_4	+0.40 / -0.40	+0.44 / -0.44

Table 5 Loprop and Mulliken charges per center at the CASSCF level (SCF for Li_4F_4) and at the CCSD(T) or CASPT2 (C_4N_4, B_4O_4 and Be_4F_4) optimized geometries.

Number of electrons in	core	lone pairs	bonds	diffuse/external orbitals
C_8	16	0	24	8
B_4N_4 [a]	15.99	7.20	22.68	2.13
Be_4O_4	15.97	7.78	24	0.25
Li_4F_4 [b]	16	31.25	0	0.75
C_4N_4	16	7.78	23.77	4.45
B_4O_4	16	7.78	24	4.22
Be_4F_4 [c]	24	0	24	4
N_8	16	15.92	24	0.09
C_4O_4 [d]	16	16	24	0.0
B_4F_4	15.99	15.97	23.92	0.13

[a] The threshold defining the core orbitals in LoProp was lowered to 1.996 instead of 1.999.

[b] At the SCF level (at the CASSCF level, there are 8 extra electrons in the core, originating from the lone pairs).

[c] LoProp failed to correctly distinguish electrons from core and lone pairs, even when thresholds were modified.

[d] The threshold defining the core has been raised to 1.99965 (from 1.999), while that for lone pairs has been raised to 1.85 (from 1.80).

Table 6 Natural bond order analysis at the CASSCF level for the optimized CCSD(T)/ANO 4s3p2d1f basis set geometries with the exception of 52-electron systems, for which the geometries are those optimized at CASPT2 level, with the same basis set.